Influence of an electrical potential on the charge transfer kinetics of bacteriorhodopsin

Christoph Kleinschmidt and Benno Hess
Max-Planck-Institut für Ernährungsphysiologie, Rheinlanddamm 201, D-4600 Dortmund 1, Federal Republic of Germany

ABSTRACT The adsorption of bacteriorhodopsin(bR)-containing purple membranes (PM) to black lipid membranes (BLM) was used to study the charge translocation kinetics of bR upon flash excitation.

The discharge of the PM-BLM system after charging upon illumination is found to proceed quite slowly (discharge time up to several minutes) but is considerably accelerated by addition of the protonophore FCCP.

Therefore, the dependence of the proton transfer kinetics in bR on electrical potentials generated by preceding flashes of varying repetition rate and intensity was investigated. The kinetics are slowed down with increasing flash intensity as well as repetition rate. This effect is partly abolished by small amounts of FCCP.

A new model is introduced which takes into account the instantaneous feedback of the electrical potential on the kinetics of the pump current. It explains the observed deviations from first-order kinetics and renders an approach with "distributed kinetics" unnecessary.

INTRODUCTION

Bacteriorhodopsin (bR) of the purple membrane (PM) of Halobacterium halobium generates a transmembrane electrochemical proton gradient upon excitation with light (for a review, see Stoeckenius et al., 1979). For the measurement of the associated pump current a net orientation of membranes is required. Several approaches are suitable for this purpose, e.g., the formation of a PM film at a water-hexane interface (Trissl and Montal, 1977), the orientation of PM in suspension by a weak electric field (Keszthelyi and Ormos, 1980) or the stabilization of an oriented PM solution by immobilization in a polyacrylamide gel (Dér et al., 1985). The use of black lipid membranes (BLM) as a support for the attachment of PM containing vesicles (Herrmann and Rayfield, 1978) or PM patches (Dancsházy and Karvaly, 1976; Bamberg et al., 1979; Fahr et al., 1981) allows the measurement of photocurrents with particular sensitivity. In the PM(patches)-BLM system, which is also used in this paper, the orientation is such that protons are pumped into the intermembranous space between PM and BLM upon excitation with light.

It is generally agreed that a net charge movement through PM is correlated with the formation of the M intermediate of the photocycle as well as with its decay to the ground state of bR (see review given in Liu and Ebrey [1988]). The time constant for the formation process is ~30 μs, for the decay several milliseconds. There is, however, poor agreement about the number of distinct translocation steps involved and the exact values of the corresponding time constants. A compilation of previously published time constants is given by Holz et al. (1988).

The question arises to which extent the photocycle or the associated pump currents in closed systems are perturbed by the membrane potential generated by charge movements. Many authors were prompted to analyze the influence of an electrochemical proton gradient across the membrane on the kinetics of bR. Quintanilha (1980) showed that it is mainly the electrical potential rather than a proton gradient which controls the decay kinetics of intermediate M whereas the rise kinetics of M was not affected. Watters et al. (1982) reported an overshoot phenomenon in the appearance of intermediate M depending on the intensity of light illumination of PM liposomes demonstrating that these systems can even show a fast feedback behavior. The coupling of the bR photocycle with an electrical potential was also suggested by Dancsházy et al. (1983) who reported a strong influence of experimental parameters like flash frequency, flash intensity, or membrane conductivity on the M decay in halobacterium cells, as well as by Groma et al. (1984) who found changes of the M decay rate in envelope vesicles depending on the intensity of background illumination.

Furthermore, there are indications that at least part of the bR pump cycle cannot be represented by a linear, sequential reaction model (Korenstein et al., 1978) or does not follow first-order kinetics with discrete exponentials as observed by Váró and Keszthelyi (1983) for the M decay kinetics in dried oriented PM samples. Groma and

0006-3495/90/09/653/11 $2.00

Dancsházy (1986) found that the number of exponentials needed for a satisfactory fit of M decay curves increases in cell envelope vesicles compared with PM sheets. The two latter papers favor a model with a continuous distribution of relaxation times rather than with discrete exponentials. Holz et al. (1988) showed that a "distributed kinetics" model on the basis of the theory of conformational substates can describe the photovoltages generated by PM attached to a BLM more adequately and in particular more reproducibly than a discrete model.

In this paper we investigate in greater detail the influence of an electrical potential built up by exciting flashes on the charge translocation kinetics in the PM-BLM system. Furthermore, a theoretical model is introduced which includes the self-inhibition of the bR pump cycle by the electrical potential generated in the course of charge translocation. We will show that this model can fully account for the observed deviations from first-order kinetics in this system.

MATERIALS AND METHODS

The experimental set-up (Fig. 1) was similar as described by Fahr et al. (1981). The membrane cell was made of teflon and equipped with quartz windows for illumination. Membranes were formed over a hole of area 0.75 mm^2 in a septum separating the two compartments (vol 1 ml each) of the cell. A small amount of membrane-forming solution (1% [wt/vol] L-1,2-diphytanoyl-3-phosphatidylcholine [Avanti Polar Lipids, Inc., Birmingham, AL] and 0.025% [wt/vol] octadecylamine [Fluka Chemie AG, Buchs, Switzerland, puriss.] in *n*-decane [99%; Sigma Chemical Co., St. Louis, MO]) was deposited at the rim of the hole. The thinning process was monitored by measurement of membrane capacity which finally reached a value of ~0.4 $\mu F/cm^2$. Membranes were usually stable for several hours. The standard buffer for measurement was 10 mM MES-KOH, pH 6.0, 150 mM KCl. The room temperature was always maintained at 20°C.

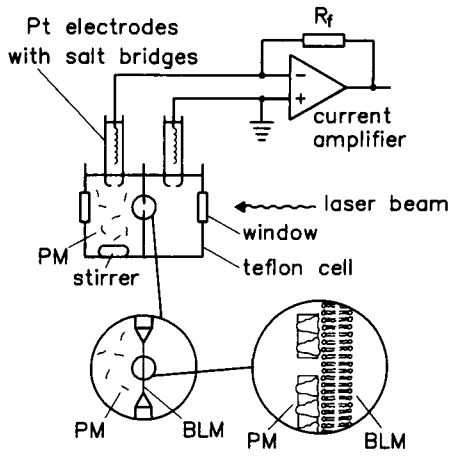

FIGURE 1 Experimental set up (schematical). See text for explanations.

Purple membrane patches were prepared from *Halobacterium halobium* (strain S9) as described (Oesterhelt and Stoeckenius, 1974). Before measurement, samples were gently sonicated for 30 s in a water bath to remove aggregates. 5 μl of a pooled PM preparation (optical density ~4 at 570 nm) were added to one compartment. After ~1 h with gentle stirring a stable electrical signal upon illumination was obtained and measurements were started. The protonophore FCCP (Carbonyl-cyanide-4-trifluoromethoxyphenylhydrazone; Serva Fine Biochemicals Inc., Garden City Park, NY) was stored in ethanolic stock solutions of 10 and 100 μg/ml and added directly to the PM containing compartment.

The membranes were illuminated with continuous light by a 100-W Hg-Lamp (LOT, Darmstadt, FRG) through an OG515 cut-off filter. Light pulses of ~10 ns half-width were generated by a frequency-doubled YAG-Laser (λ = 532 nm; model YG481; Quantel, Orsay, France) and the intensity was adjusted by neutral density filters. We used a fiber optics cable to guide the laser light onto the membrane. Flash intensities were measured by a Joulemeter (model Rj-7100; Laser Precision Corp., Utica, NY), and ranged between 22 $\mu J/cm^2$ and 2.4 mJ/cm^2.

Platinized platinum electrodes, connected by a salt bridge to the compartments, were used. As current amplifier we used either a Keithley model 427 with variable gains between 10^8 and 10^{10} V/A and a selectable risetime (minimum ~10 μs) or a home-made low-noise current voltage converter using op-amps AD-OP37 (gain 10^7 V/A, risetime ~400 ns). A simple electrical switch allowed a fast change of the amplifiers.

The measurement of currents over the whole time range accessible with the BLM method is hampered by the mutual dependence of the time constant and the current amplitude of each charge translocation step. Because the integral of current with time represents the transferred charge (which is of the same magnitude for each step), the amplitudes of slow steps are rendered very small and are lost in the amplifier noise. One way to circumvent this problem is the measurement of photovoltages instead of currents (Holz et al., 1988). The other possibility, which we employed in this work, is the recording of currents with different amplifier gains one after another. We generally performed two measurements, the first with 10^7 V/A (risetime 400 ns), the second with 10^8 V/A (risetime 30 μs). With an appropriate choice for the time base settings of the recording oscilloscope we span by this procedure a time window from ~1 μs up to 0.5 s, with a large overlap of both sections.

The amplifier output was stored in a digital storage oscilloscope (model 9400A; LeCroy, Chestnut Ridge, NY) with 25,000 data points and a vertical resolution of 8 bits. Summation averaging of successive flashes was possible. Data were then stored in a personal computer and condensed by a procedure which simulates a logarithmic time base and averages the data between the calculated time points.

The data were subsequently transferred to a Convex 201 vector processor and evaluated with a self-written program (based on the model described in the appendix) utilizing the least square fitting routine VA05AD of the HARWELL subroutine library (Theoretical Physics Division, A.E.R.E., Harwell, UK). The model to be fitted cannot be given in an explicit form but is represented by the differential Eq. A9 which was solved for each iteration step over the whole time range by the fourth-order Runge-Kutta method. This rendered the procedure very time consuming and executable only on a fast computer. Always two measurements with different current sensitivities and different time

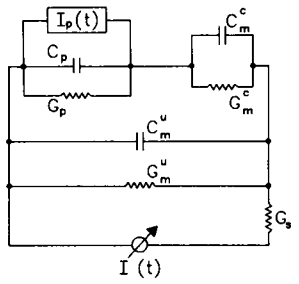

FIGURE 2 Equivalent circuit of the arrangement shown in Fig. 1.
$I_p(t)$: Pump current
$I(t)$: Current measured in the external circuit
C_p,G_p: Capacitance and conductance of purple membrane
C^c_m, G^c_m: Capacitance and conductance of the covered part of the BLM
C^u_m, G^u_m: Capacitance and conductance of the uncovered part of the BLM
G_s: Conductance of the external circuit, including electrodes and aequous solutions

resolutions (see above) were fitted together with the same set of parameters.

Equivalent circuit of the experimental set-up

To define the electrical parameters which govern the time behavior of the measuring set up, we show in Fig. 2 the electrical equivalent circuit of the PM-BLM system used in this work. This set up allows an undisturbed measurement of the time course of charge translocation in a certain time window (Fahr et al., 1981). The window limits are given on the fast side by a passive system time constant ($\tau = (C^u_m + C^c_m)/G_s$), which is ~3 μs under our conditions ($C_m = C^u_m + C^c_m \approx 3$ nF, $1/G_s \approx 1{,}000\ \Omega$) and on the slow side by the onset of proton flows through the conductivities G_p and G^c_m which are both (at least principally) affected by the addition of protonophores.

A slight simplification is made in Fig. 2 in that the Pt electrodes actually do not allow the passage of electrons to the solutions and thus should be ac coupled. However, we omitted these additional capacitances because they are in the order of ~10 μF (Liu and Ebrey, 1988) and discharge through the very large BLM resistance. Hence, the current traces should not be distorted by these capacitors even in the time range of seconds.

RESULTS

1. Charging and discharging of the membrane system

When illumination of the PM-BLM system with continuous light is suddenly initiated by a camera shutter, the pumping of protons into the intermembraneous space between PM and BLM is triggered and yields a large transient current, which soon declines to the baseline level indicating an almost complete inhibition of the pump by the resulting electrochemical proton gradient (Bamberg et al., 1979). Upon addition of a proton-conducting chemical like FCCP, a steady-state current is observed demonstrating that protons can now flow through the BLM thereby abolishing the inhibition of the pump (Fig. 3).

To monitor the discharge of the membrane system after switching off the continuous illumination, we modified these experiments in the following way: the membranes were irradiated for 2 min by strong continuous green-yellow light to produce a saturating proton density in the intermembranous space. After switching off the light the membranes were allowed to discharge in the dark for a certain time t. After that time the shutter was opened again and the resulting peak current I_{peak} (see Fig. 3 for definition) was measured. Because residual charges between the two membranes diminish I_{peak} by an inhibition of the pump activity, the intermembranous charge density at time t after the end of illumination can be monitored qualitatively and by variation of the dark time t the discharge of the system can be followed. The time resolution of this method is ~1 s.

The results shown in Fig. 4 demonstrate that without addition of FCCP the peak current relaxes to the value without inhibition with a characteristic time constant of ~50 s. The time course was not exactly the same for every membrane preparation. In some cases we observed changes of I_{peak} up to 600 s. Addition of protonophore leads to an increase in peak height due to the reduced self-inhibition of the proton pump. Simultaneously, the discharge process is considerably accelerated and its early parts can no longer be resolved. Because FCCP enhances specifically the proton conductivity of lipid bilayer membranes, these observations clearly indicate that residual protons in the intermembraneous space are responsible for the inhibition.

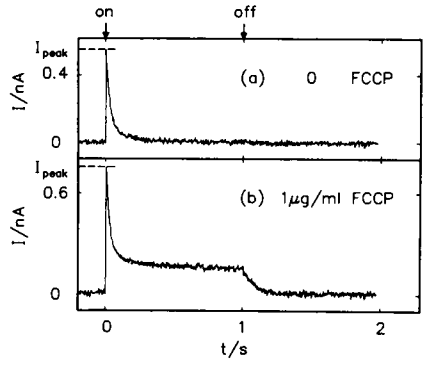

FIGURE 3 (*a*) Photocurrent response upon irradiation with continuous light (100-W Hg-lamp with 515-nm cut-off filter). Light intensity ~1 mW/cm^2. (*b*) Same as *a* after addition of 1 μg/ml FCCP.

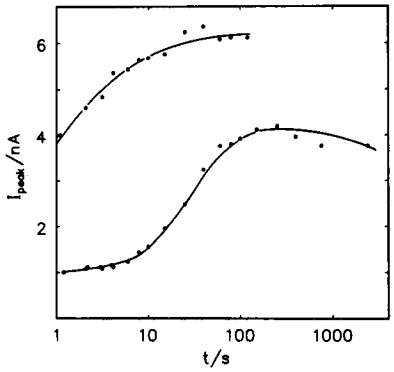

FIGURE 4 Initial peak current as a function of the dark time t. Illumination with 515-nm cut-off filter (~5 mW/cm^2). (*Lower curve*) Without protonophore. (*Upper curve*) After addition of 1 μg/ml FCCP.

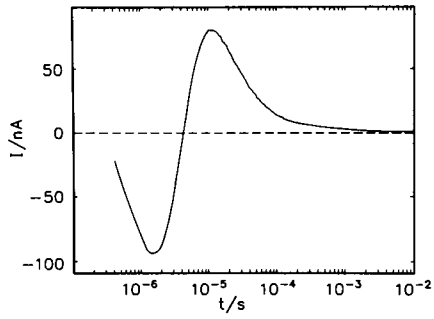

FIGURE 5 Fast part of photocurrents after flash excitation. Area of BLM: 0.75 mm^2. Buffer: 10 mM MES-KOH pH 6.0, 150 mM KCl. T = 20°C. The signal is an average over 25 laser flashes of energy 70 μJ/cm^2, λ = 532 nm, flash repetition rate 0.1 Hz. FCCP concentration: 0.2 μg/ml.

2. Qualitative measurements of charge translocation kinetics: influence of flash intensity, flash frequency, and membrane conductivity

Because the discharge of the PM-BLM system proceeds quite slowly, an interference of the electrical potential generated by residual charges with the pump process is expected, when repetitive flash excitation of PM is employed. Therefore, we investigated the influence of experimental parameters, which determine the build-up and the decay of a membrane potential, flash intensity, flash frequency, and membrane conductivity, on the charge transfer kinetics in bR.

Because it is known from many experiments that proton translocation in bR comprises at least three steps with time constants in the range from 10 μs up to some milliseconds (Holz et al., 1988), we examined the whole accessible time range for alterations in the pump current kinetics. The following measurements are recordings of the translocation current $I(t)$ as a function of the time t after an exciting laser flash.

Fig. 5 shows the current signal for the first part of the time window. Up to ~10 μs the trace is mainly governed by the amplifier rise time (400 ns) and the time constant of the BLM measuring system (~3 μs). The negative amplitude of the current in this early time range, which is spectroscopically connected with the bR → J → K → L transitions, points to a charge motion opposite to the overall pump direction. An assignment of the negative current to one single of these transitions is not possible due to the limited time resolution of the measuring system. The large positive lobe between 10^{-5} and 10^{-4} s is commonly attributed to the L → M transition in the bR photocycle. We found that the current trace in this time region is hardly affected by a change of parameters which influence the electrical potential conditions (see quantitative evaluation below) indicating a rather small dependence of the activation barrier of the L → M transition on the electrical field. Therefore, we focus in the following on the current trace between 1 ms and ~0.1 s, the time range which turned out to be most sensitive to external parameters.

Fig. 6 shows the influence of flash repetition rate on the translocation current, displayed in a double-logarithmic plot. Increasing the time interval between successive flashes enhances the current amplitude and simultaneously speeds up the charge movement which results in an intersection of the traces at ~300 ms. Note the appearance of a marked shoulder in the current trace between 10^{-2} and 10^{-1} s for high repetition rates. We

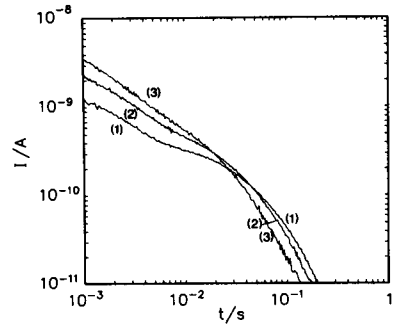

FIGURE 6 Double-logarithmic plot of current vs. time for different laser flash repetition rates. (1) f = 0.5 Hz, 200 flashes; (2) f = 0.1 Hz, 70 flashes; (3) f = 0.01 Hz, 20 flashes. All other conditions were the same as in Fig. 5 except that no FCCP was added. The three curves were recorded using the same membrane. The fact that the noise does not increase for lower current values is a mere consequence of averaging more data points in later time stages.

observed kinetic differences for flash intervals up to 500 s. However, if FCCP is added they are markedly diminished though not completely abolished. A concentration as small as 0.2 μg/ml FCCP is sufficient to accomplish this (data not shown).

In Fig. 7 the currents generated by different laser flash intensities are plotted. Besides the expected differences in amplitude, again modifications in kinetics appear. A characteristic shoulder between 0.01 and 0.1 s for high intensities is again found. We observed a similar influence of the flash intensity on the pump kinetics for all flash frequencies (down to 0.002 Hz) and all FCCP concentrations applied indicating that not so much the initial state at the time of the exciting flash as rather the formation of an electrical potential in the course of charge translocation is responsible for these effects. This suggests an evaluation procedure which takes into consideration the changing of relaxation times during the process itself according to the build-up of an electrical potential.

In Fig. 8 the influence of membrane conductivity as controlled by the FCCP concentration is displayed. Without FCCP, again the shoulder between 0.01 and 0.1 s can be seen. Upon addition of a very small amount of protonophore, this shoulder disappears while the amplitude rises. However, this picture changes if more protonophore is added (curve 3 in Fig. 8). The initial amplitude does not rise further (compare currents at 1 ms) but a large lobe appears at ~0.1 s, which is caused by a discharge of the PM-BLM membrane system. This discharge current adds to the undisturbed pump kinetics and makes a more than qualitative evaluation of data impossible (at least for times >0.01 s after the flash).

Another way to look at the interaction of FCCP with the membrane system is the direct recording of the current backflow after the proton pump translocation. This is shown in Fig. 9 for different FCCP concentrations.

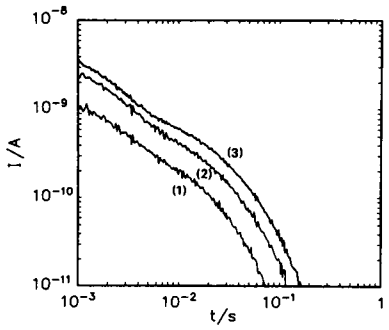

FIGURE 7 Double-logarithmic plot of current vs. time for different laser flash intensities. Flash repetition rate 0.1 Hz, no FCCP added. Each curve is an average over 25 flashes. Flash energies: (1) 22 μJ/cm², (2) 70 μJ/cm², (3) 120 μJ/cm². All other conditions were the same as in Fig. 5. The three curves were recorded using the same membrane.

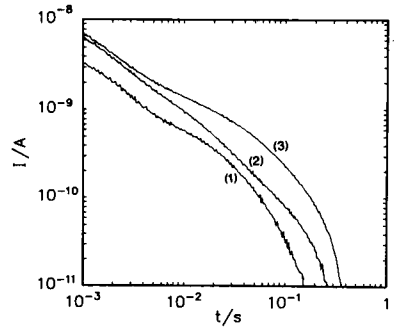

FIGURE 8 Double-logarithmic plot of current vs. time for different concentrations of protonophore. Flash repetition rate 0.1 Hz, flash energy 120 μJ/cm². Each curve is an average over 25 flashes. FCCP concentrations: (1) 0, (2) 0.2 μg/ml, (3) 0.5 μg/ml. All other conditions were the same as in Fig. 5. The three curves were recorded using the same membrane.

Note the different time scale and the range of currents which is lower than that in the previous figures. Without FCCP a net backflow of charges is observed, represented by a negative discharge current. After addition of FCCP this current gradually turns positive demonstrating a discharge in the direction of proton pumping through the BLM. Thus, Fig. 9 shows again that with increasing membrane conductivity considerable discharge currents occur and have to be considered in addition to changes due to a relaxation of the membrane potential.

3. Data evaluation with a new model allowing for potential formation during translocation

The qualitative results shown in 2. demonstrate that a reasonable theoretical model for these experiments should

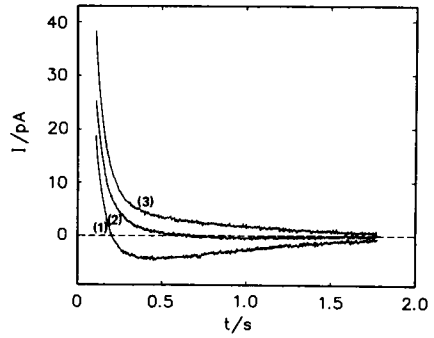

FIGURE 9 Current traces for the last part of the reaction. Flash repetition rate 0.1 Hz, flash energy 70 μJ/cm², amplifier gain 10^{10} V/A. (1) 60 flashes, no FCCP added, (2) 90 flashes, 0.5 μg/ml FCCP, (3) 100 flashes, 1.0 μg/ml FCCP. All other conditions were the same as in Fig. 5. The three curves were recorded using the same membrane.

allow for changes in membrane potential and thus for variations in relaxation times during the time course of charge translocation. We therefore developed a model in which the sharply defined relaxation time of a charge translocation step is replaced by the band between an "initial" lifetime corresponding to the starting electrical potential and a "final" lifetime which is enlarged by the increased field. This band is run through according to an exponential dependence of the relaxation time on the membrane potential (Läuger, 1984), which in turn is determined by the progressive charge translocation. The derivation of this model is given in the appendix.

In Fig. 10 one example of a current trace measured over the full time range is shown together with the result of the fit according to our model. The fit was done assuming three translocation steps. The introduction of a fourth step did not improve the quality of the fit. No satisfactory fit was obtained with only two steps.

It turned out that three distinct translocation steps were in all cases sufficient to fit the experimental data. Table 1 shows the determined parameters for different laser flash intensities and FCCP concentrations. It should be emphasized again that $\tau_i(0)$ is the relaxation time of step i at the beginning of this step but after completion of step i − 1. Likewise, $\tau_i(\infty)$ is the final lifetime of step i before the onset of step i + 1. An error analysis for the calculated parameters was done by linearization of the model around the minimum of the sum of squares using the inverse Hessian matrix at that point. The resulting confidence limits are given in Table 1 and should be regarded as estimations.

In Fig. 11 the data are graphically represented without specification of the errors. The results can be summarized as follows: the first relaxation time, which is commonly

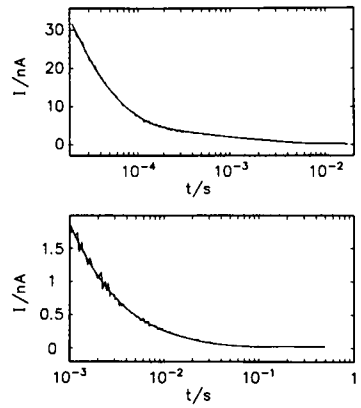

FIGURE 10 Example of photocurrent traces, recorded over the full time range. The two curves were measured with different amplifiers directly one after another. Flash repetition rate 0.1 Hz, flash energy 22 $\mu J/cm^2$, FCCP concentration 0.2 $\mu g/ml$. (*Upper panel*) Average of 25 flashes, gain 10^7 V/A, risetime 400 ns. (*Lower panel*) Average of 50 flashes, gain 10^8 V/A, risetime 30 μs. All other conditions were the same as in Fig. 5. The data were fitted according to Eqs. A12 and A9 with the number of translocation steps $n = 3$. The smooth lines are the result of the fit, which was done for both curves simultaneously with the same set of parameters. The fitting started at 20 μs and 1 ms, respectively. The large overlap between 10^{-3} and 10^{-2} s ensures a proper transition between the two sections. The numeric results can be found in the respective line of Table 1.

attributed to the L → M transition is confined to values between 10 and 30 μs. There is no strong influence of flash intensity or FCCP concentration on $\tau_1(0)$ and $\tau_1(\infty)$.

The second time constant, which is difficult to assign to known intermediates, shows a marked decrease upon addition of a very small amount of protonophore. Simultaneously, the range run through by this relaxation time

TABLE 1 Time constants and displacement coefficients of bR attatched to BLM

Concentration of FCCP	Laser flash intensity	$\tau_1(0)$	$\tau_1(\infty)$	α_1	$\tau_2(0)$	$\tau_2(\infty)$	α_2	$\tau_3(0)$	$\tau_3(\infty)$	α_3*
μg/ml	*μJ/cm²*	*μs*	*μs*		*ms*	*ms*		*ms*	*ms*	
0	120	9.4 ± 0.2	30.2 ± 0.8	0.18 ± 0.01	0.54 ± 0.01	0.82 ± 0.06	0.20 ± 0.01	11.0 ± 0.5	20.1 ± 3.2	0.62
	70	11.5 ± 0.5	28.9 ± 1.7	0.15 ± 0.01	0.65 ± 0.03	0.80 ± 0.09	0.22 ± 0.01	8.5 ± 0.8	18.4 ± 4.9	0.63
	22	10.4 ± 0.6	31.4 ± 2.6	0.14 ± 0.01	0.69 ± 0.07	0.94 ± 0.20	0.23 ± 0.01	7.9 ± 1.1	11.4 ± 3.5	0.63
0.2	120	9.7 ± 0.1	25.7 ± 0.7	0.13 ± 0.01	0.30 ± 0.02	0.59 ± 0.02	0.15 ± 0.01	5.8 ± 0.4	91 ± 58	0.72
	70	10.0 ± 0.2	24.5 ± 1.2	0.17 ± 0.01	0.27 ± 0.03	0.52 ± 0.10	0.21 ± 0.01	3.0 ± 0.6	9.8 ± 1.9	0.62
	22	10.7 ± 0.4	26.6 ± 1.8	0.16 ± 0.01	0.34 ± 0.05	0.60 ± 0.15	0.24 ± 0.01	3.3 ± 0.9	8.6 ± 2.0	0.60
0.5	120	13.6 ± 0.2	25.3 ± 0.8	0.08 ± 0.01	0.25 ± 0.01	1.00 ± 0.13	0.15 ± 0.01	11.7 ± 0.4	74 ± 23	0.77
	70	14.5 ± 0.3	28.5 ± 1.5	0.11 ± 0.01	0.27 ± 0.04	0.74 ± 0.20	0.16 ± 0.01	5.3 ± 0.6	20.3 ± 4.5	0.73
	22	16.4 ± 0.4	25.2 ± 1.4	0.10 ± 0.01	0.30 ± 0.04	0.75 ± 0.23	0.18 ± 0.01	5.3 ± 0.7	16.2 ± 3.2	0.72
1.0	120	12.8 ± 0.2	28.3 ± 1.2	0.08 ± 0.01	0.25 ± 0.01	0.96 ± 0.08	0.14 ± 0.01	12.4 ± 0.4	47.7 ± 8.9	0.78
	70	14.6 ± 0.3	32.5 ± 1.4	0.08 ± 0.01	0.31 ± 0.01	0.68 ± 0.06	0.12 ± 0.01	9.4 ± 0.5	51.6 ± 16.4	0.80
	22	15.1 ± 0.7	34.4 ± 4.9	0.07 ± 0.01	0.30 ± 0.05	0.59 ± 0.11	0.11 ± 0.01	8.1 ± 1.2	73 ± 44	0.82

*α_3 was calculated from $\alpha_3 = 1 - \alpha_1 - \alpha_2$ and thus given without error.

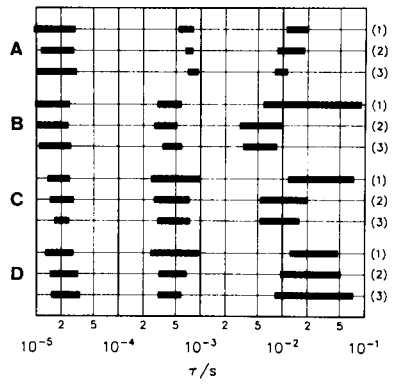

FIGURE 11 Graphical representation of the results from Table 1. The left and right edge of each bar denote the initial and the final relaxation time of the respective step. The confidence limits specified in Table 1 are omitted for clarity. The concentration of FCCP is 0 (*A*), 0.2 μg/ml (*B*), 0.5 μg/ml (*C*), 1.0 μg/ml (*D*). Flash intensities: 120 $\mu J/cm^2$ (1), 70 $\mu J/cm^2$ (2), 22 $\mu J/cm^2$ (3).

becomes larger. Increasing flash intensities also tend to broaden the band width of the lifetime. All these findings support our interpretation that the variability of lifetimes originates from the electrical potential.

Similar statements can be made for the third relaxation time which belongs to the decay from M to bR. The band width increases with FCCP concentration and with flash intensity (with the exception of the highest FCCP concentration). Moreover, $\tau_3(0)$ rises with light intensity, reflecting the generation of electrical potentials by steps 1 and 2 and/or by preceding flashes. The dependence of $\tau_3(0)$ on FCCP concentration shows first a strong decrease upon addition of 0.2 μg/ml protonophore (from ~10 to ~3 ms), which can be explained by an almost complete discharge of the membrane system during the flash repetition interval. With higher concentrations, however, $\tau_3(0)$ rises again. Simultaneously, the relative displacement coefficient α_3 (cf. Table 1) increases. These findings indicate that now a substantial discharge current flows through the BLM and adds to the pure pump kinetics. Strictly speaking, our model of evaluation is no longer applicable because a new proton pathway (which does not belong to the bR pump cycle) appears. Because it is obviously not possible to separate this discharge current from step 3 quantitatively we do not extend the model by the new translocation process but emphasize the limited applicability of the 3-step model to high BLM conductivities. Therefore, only at low FCCP concentrations the fitted model parameters τ_i and α_i in Table 1 can be taken as the real molecular constants. E.g., it may not be concluded from the values for the α_i in Table 1 that the physical displacement lengths are dependent on the FCCP concentration. The rise of α_3 with the FCCP concentration is a consequence of the increasing contribution of discharge currents and is accompanied by a corresponding decrease of α_1 and α_2.

Finally, we extract from Table 1 the smallest initial and final values of the relaxation times to give the best approximation to the potential-free case. These results are:

Step 1: ~10–30 μs

Step 2: ~300–560 μs

Step 3: ~3–9 ms

Additionally, from the first six measurements in Table 1, we gather the average displacement coefficients: α_1 = 15%, α_2 = 21%, α_3 = 64%.

DISCUSSION

The PM-BLM structure as a closed system

Bacteriorhodopsin in purple membrane is an extremely tightly packed membrane protein with a density of $\sim 1 \cdot 10^{13}$ molecules per cm^2 (Henderson and Unwin, 1975). A simple calculation illustrates the power of PM to generate a membrane potential: if only 10% of the bR molecules are excited and pump one single proton each, the translocated charge is $Q = 1.6 \cdot 10^{-19} \cdot 0.1 \cdot 1 \cdot 10^{13}\ C/cm^2 = 1.6 \cdot 10^{-7}\ C/cm^2$. With an estimated PM capacity C_m of ~2 $\mu F/cm^2$ we obtain a transmembrane voltage of $U = Q/C_m \approx 80$ mV. Of course, the voltage will be lower in membrane systems, where PM makes up only a small part of the whole membrane, as e.g., in vesicles or in bacterial cells. But when purified PM is used and when a fast backflow of charges is prevented by the experimental conditions, the build-up of an electrical potential due to a single flash excitation can no longer be neglected. The measurement of currents in the PM-BLM sandwich structure represents such an experimental situation.

When the supply of energy is stopped, a closed system becomes slowly deenergized with time. As shown in Fig. 4, the discharge process in the PM-BLM sandwich structure is also found to be quite slow. An additional quantitative analysis (not shown) of the data of Fig. 4 reveals that the relaxation of I_{peak} does not follow a first-order kinetics as would be expected for a voltage independent conductivity $G_m^c + G_p$ (cf. Fig. 2) but contains at least two time constants between 1 and 100 s. Moreover, as shown in Fig. 9, a current backflow can already be detected ~0.2 s after a flash excitation. However, because the quantitative relation between I_{peak} and the state of charging is not known, a single-exponential decay of the intermembraneous charge density cannot be ruled out completely. In any case, the

representation of the intermembraneous space by the plates of electrical capacitors is an oversimplification. Protonatable groups in this space can be occupied and show saturation behavior. Moreover, the binding of PM sheets to the BLM is likely to be loosened by a high charge density thus rendering G_p voltage dependent.

The data of Fig. 9 show that without FCCP the discharge process proceeds mainly through the PM (or the junction between PM and BLM), which results in a negative discharge current. As seen from curve 3, the addition of protonophores has a larger effect on the BLM conductivity than on the PM conductivity thus making the discharge current positive (in the direction of proton pumping). Apparently, the quasi-crystalline structure of purple membrane makes it less accessible for small molecules like FCCP than a normal lipid bilayer membrane.

Interference of residual charges with the pumping process

From the results given in Figs. 6–8 the following conclusions can be drawn. Because the flash repetition rate controls the amount of remaining charges at the time of the next flash, the data in Fig. 6 demonstrate that these charges influence the kinetics over the full time range of τ_2 and τ_3. Contrarily, addition of protonophore causes the system to be always in the same initial state (for flash intervals $\geq$10 s), hence the near abolishment of the influence of the flash repetition rate can be easily explained.

Under repetitive flash excitation, the PM-BLM system is in a quasi-stationary state, where the charges flowing back between two successive flashes equal the charges translocated during the pump cycle after excitation. Thus, during charging an electrical potential inside the membrane runs through the same values as during discharging, although in reversed order. Because the pump kinetics depend markedly on the initial state of charging which is determined by the flash repetition rate (as shown in Fig. 6), the suggestion is plausible that the time constants of the bR reaction sequence are changed continuously during the charging process after a single flash excitation.

The intensity of an exciting flash affects not only the current amplitudes but also the kinetics of charge translocation (Fig. 7). This could be explained exclusively by different initial states due to different amounts of residual charges. However, the fact that influences of light intensity are observed even at flash repetition rates as low as 0.002 Hz, where the system is almost completely relaxed at the time of the next flash (cf. Fig. 4), supports our notion that the electrical potential built up during the charge translocation after a flash excitation also directly feeds back on its generating current.

The addition of FCCP (Fig. 8) leads at concentrations not larger than 0.2 μg/ml (corresponding to ~0.8 μM) to an improvement of the experimental situation in that the discharge process is now fast enough to reduce the membrane potential considerably during the time interval between two successive flashes (here: 10 s) but still too slow to perturb the charge movements coupled with the bR pump cycle ($t \leq 200$ ms after a flash).

Restrictions in measurement time due to the limited lifetime of a BLM do not allow us to give a more precise value for the optimal FCCP concentration, where the effects of the electrical potential are minimized without severe disturbance of the pump current by fast discharge processes. Moreover, because small variations in BLM constitution certainly affect the conductivity increase upon protonophore addition, this optimum should be determined for each new membrane preparation. Qualitatively, we observed always the same behavior as shown in Fig. 8.

Conclusions from the numerical evaluation: membrane potential effects vs. distributed kinetics

Holz et al. (1988) also used the PM-BLM system to study the charge translocation in bR but measured photovoltages instead of photocurrents. For evaluation they applied the concept of "distributed kinetics" (Austin et al., 1975) which assumes a protein intermediate to consist of a set of conformational substates and consequently leads to a distribution of activation energies E_A for the reactions of this intermediate. The kinetic constants are regarded to follow the Arrhenius equation $k = A \cdot \exp(-E_A/RT)$.

Holz et al. (1988) furthermore assumed the distribution function $g(E_A)$ of activation energies to be Gaussian and found a satisfactory fit of their kinetic data with three continuous bands with the following peak rate constants: $\tau_1 = 32 \pm 8$ μs, $\tau_2 = 0.89 \pm 0.15$ ms, $\tau_3 = 18 \pm 5$ ms (in 150 mM KCl, pH 7.0 at 25°C) with $\alpha_1 = 20\%$, $\alpha_2 = 15\%$, $\alpha_3 = 65\%$. These values were determined without adding protonophores and agree very well with the corresponding results of our study.

Two conclusions can be drawn from this agreement. First, photovoltage and photocurrent measurements yield principally the same results and are equivalent in that sense. However, both methods have their special advantages. With photovoltage measurements the problem of small amplitudes is avoided and uninterrupted recordings through the whole time range are possible. On the other hand, the addition of a protonophore increases the BLM conductivity and leads to a fast breakdown of the voltage to be measured. Only photocurrent measurements thus

allow a systematic investigation of protonophore effects as performed in this study.

Secondly, both underlying mathematical models, although starting from completely different ideas, give similar figures for the relaxation times and their amplitudes. This is not surprising because the main feature of both approaches is the consideration of whole bands of time constants. The main difference lies in the fact that in the distributed kinetics approach all time constants in a band are present simultaneously whereas our model assumes the lifetimes to run through their range according to the increasing potential. As demonstrated by our results, this difference has no drastic consequences for the numeric values. Hence, we can state that our model can account for the observed deviations from first-order-kinetics in the PM-BLM system and makes it unnecessary to invoke "distributed" kinetics. Furthermore, our experiments with FCCP show that the inhibition of the pump process by electrical potentials is indeed important in this system and must not be disregarded in the numerical evaluation.

Comparison with photocycle data

Dancsházy et al. (1983) determined the time constant of the M decay in Halobacterium cells as a function of flash intensity, flash frequency, and uncoupler concentration. They found the decay time constant to vary in the range between 3 and 16 ms, which is in good agreement with the figures for τ_3 in our work. Moreover, the limit value for low flash intensity and for high uncoupler concentration in this work (3–4 ms) also agrees with our data. Finally the experimentally determined dependence of the M decay time on the membrane potential (Fig. 5 *B* in Dancsházy et al. [1983]) indicates an exponential law as it was assumed for the interpretation of our data.

An extensive investigation of the photocycle kinetics in a PM suspension was done by Xie et al. (1987). Here influences of electrical potentials are not expected to occur. For the purpose of comparison we therefore use our minimal values of the initial relaxation times $\tau_i(0)$. Our figures for $\tau_2(0)$ and $\tau_3(0)$ (300 μs and 3 ms) are also present in the relaxation time spectrum of the photocycle (Xie et al., 1987, indices 3 and 7, respectively). Another time constant in the quoted paper (index 2, $\tau_2 = 23$ μs) is slightly higher than our $\tau_1(0)$, but fits well in the observed range between 10 and 30 μs.

An even better confirmation of our data comes from a work which fits together the data from photocycle investigations, infrared experiments, and measurements of electrical currents in gels (Müller, K. H., H. J. Butt, E. Bamberg, K. Fendler, B. Hess, F. Siebert, and M. Engelhard, personal communication). In the range between 10 μs and 5 ms these authors find four relaxation times of which the second (~250 μs) and the fourth (~3 ms) correspond very well to our larger time constants. Moreover, the third time constant in this study (~1 ms) is not found when the electrical data are fitted alone. The fastest relaxation time (~40 μs) is again larger than that found in our work.

Relating the observed kinetic constants to known intermediates in the photocycle is difficult. We only can state that the fast translocation step (10–30 μs) is closely coupled to the formation of M and the slowest step (~3 ms) takes place during the decay of M to the groundstate of bR. The assignment of the second step (~300 μs) is still open. Of course, measured time constants are always apparent and may not be mistaken as the intrinsic constants associated with detailed models including back reactions and possible branching.

APPENDIX

Derivation of a model including feedback of an electrical potential on its generating photocurrent

Without consideration of electrical potential effects, the measurable current caused by a linear sequence of n distinct charge translocation steps is given by (Fahr et al., 1981)

$$I(t) = \sum_{i=1}^{n} a_i \exp(-t/\tau_i), \tag{A1}$$

where τ_i is the (time-independent) relaxation time of step i. For the charge translocated in step i follows

$$Q_i = \int_0^\infty a_i \exp(-t/\tau_i)\, dt = a_i\tau_i = Ne_0\alpha_i, \tag{A2}$$

where N is the number of excited bR molecules, e_0 the elementary charge, and α_i a dimensionless displacement coefficient which is the ratio between the displacement length l_i and the total membrane thickness d_0:

$$\alpha_i = l_i/d_0. \tag{A3}$$

Eq. A1 is no longer valid if the τ_i are considered to be time-dependent. For the derivation of a more adequate description we first restrict ourselves to one single step i of the reaction.

First we have to introduce a model dependence of the relaxation time τ_i upon the (time-dependent) membrane potential. We essentially use an equation given by Läuger (1984), which is based on the theory of absolute reaction rates:

$$\tau_i(t) = \tau_i(0) \exp \frac{\Delta U_i(t)}{2kT}, \tag{A4}$$

where $\tau_i(0)$ is the relaxation time at time zero (not necessarily at potential zero) and ΔU_i is the additional voltage drop at time t (in relation to the reference state at time zero) over the length of translocation step i. k is Boltzmann's constant, T is the absolute temperature. We consider $\Delta U_i(t)$ to be proportional to the total membrane potential $U(t)$. Lumping all constants together we obtain

$$\tau_i(t) = \tau_i(0) \exp[k_i' U(t)], \tag{A5}$$

where $U(t)$ is the additional membrane potential with respect to the reference state at time zero. k_i' is a constant. A further assumption in our model is that the rise of $U(t)$ which has to be used in Eq. A5 is only due to currents produced by step i itself, i.e., we neglect any influence of other steps on the time course of $U(t)$. This assumption is justified, if $\tau_i(t) \gg \tau_{i-1}(t)$ for all t, i.e., if step i − 1 is almost completely finished before a significant onset of step i. The results will show that this is indeed the case. Thus the steps following and those preceding step i do not feed back to step i. However, the latter modify the reference state, i.e., the initial time constant $\tau_i(0)$.

Under this assumption follows that $U(t)$ in Eq. A5 is proportional to the already transferred fraction $y_i(t)$ of charges in step i: $U(t) \sim y_i(t)$, where $0 \le y_i(t) \le 1, y_i(0) = 0, y_i(\infty) = 1$. With Eq. A5 we obtain

$$\tau_i(t) = \tau_i(0) \exp [k_i'' y_i(t)] \tag{A6}$$

and

$$\tau_i(\infty) = \tau_i(0) \exp k_i'', \tag{A7}$$

k_i'' being a constant. Combination of Eqs. A6 and A7 yields:

$$\tau_i(t) = \tau_i(0) \left(\frac{\tau_i(\infty)}{\tau_i(0)}\right)^{y_i(t)}. \tag{A8}$$

The rate equation for step i can now be written as usual, but with a time-dependent rate constant $k_i(t) = 1/\tau_i(t)$:

$$\frac{dy_i}{dt} = k_i(t) \cdot [1 - y_i(t)] = [1 - y_i(t)]/\tau_i(t)$$

$$= \frac{1 - y_i(t)}{\tau_i(0) \cdot \left(\frac{\tau_i(\infty)}{\tau_i(0)}\right)^{y_i(t)}} \tag{A9}$$

with the initial condition $y_i(0) = 0$. Differential Eq. A9 cannot be solved analytically.

The pump current $I_i(t)$ associated with step i is proportional to $dy_i(t)/dt$. The proportionality constant can be found by calculating the current integral, which equals $Ne_o\alpha_i$ (compare Eq. A2) and using the condition

$$\int_0^\infty \frac{dy_i}{dt}\, dt = y(\infty) - y(0) = 1. \tag{A10}$$

The result reads:

$$I_i(t) = Ne_o\alpha_i \cdot \frac{dy_i}{dt}(t) \tag{A11}$$

and the total pump current is

$$I_p(t) = \sum_{i=1}^{n} I_i(t) = Ne_o \sum_{i=1}^{n} \alpha_i \frac{dy_i}{dt}(t), \tag{A12}$$

where $dy_i/dt\ (t)$ is the solution of Eq. A9.

The measurable current $I(t)$ is directly proportional to the pump current $I_p(t)$ (Fahr et al., 1981). The proportionality constant, however, is not known precisely. Therefore, the total amplitude of $I(t)$ is not related to a physically significant parameter. Fitting Eq. A12 to a measured current curve thus means the adjustment of $3n - 1$ parameters:n initial lifetimes $\tau_i(0)$, n final lifetimes $\tau_i(\infty)$, and $n - 1$ independent displacement coefficients α_i (because $\Sigma_{i=1}^{n} \alpha_i = 1$).

We thank Mr. H. Schlüter for the design of the fast current amplifier and Mr. K. H. Müller for help with the fitting procedures. Thanks are also due to Drs. M. Engelhard and D. Kuschmitz for many useful discussions and Dr. E. Bamberg for valuable help with regard to the experimental set up.

This work was supported by the Stiftung Volkswagenwerk.

Received for publication 18 December 1989 and in final form 2 May 1990.

REFERENCES

Austin, R. H., K. W. Beeson, L. Eisenstein, H. Frauenfelder, and I. C. Gunsalus. 1975. Dynamics of ligand binding to myoglobin. *Biochemistry.* 14:5355–5373.

Bamberg, E., H.-J. Apell, N. A. Dencher, W. Sperling, H. Stieve, and P. Läuger. 1979. Photocurrents generated by bacteriorhodopsin on planar bilayer membranes. *Biophys. Struct. Mech.* 5:277–292.

Dancsházy, Zs., and B. Karvaly. 1976. Incorporation of bacteriorhodopsin into a bilayer membrane; a photoelectric-spectroscopic study. *FEBS (Fed. Eur. Biochem. Soc.) Lett.* 72:136–138.

Dancsházy, Zs., S. L. Helgerson, and W. Stoeckenius. 1983. Coupling between the bacteriorhodopsin photocycle kinetics and the protonmotive force. I. Single flash measurements in *Halobacterium halobium* cells. *Photobiochem. Photobiophys.* 5:347–357.

Dér, A., P. Hargittai, and J. Simon. 1985. Time-resolved photoelectric and absorption signals from oriented purple membranes immobilized in gel. *J. Biochem. Biophys. Methods.* 10:295–300.

Fahr, A., P. Läuger, and E. Bamberg. 1981. Photocurrent kinetics of purple membrane sheets bound to planar bilayer membranes. *J. Membr. Biol.* 60:51–62.

Groma, G. I., and Zs. Dancsházy. 1986. How many M forms are there in the bacteriorhodopsin photocycle? *Biophys. J.* 50:357–366.

Groma, G. I., S. L. Hélgerson, P. K. Wolber, D. Beece, Zs. Dancsházy, L. Keszthelyi, and W. Stoeckenius. 1984. Coupling between the bacteriorhodopsin photocycle kinetics and the protonmotive force in Halobacterium halobium cell envelope vesicles. II. Quantitation and preliminary modeling of the M → bR reactions. *Biophys. J.* 45:985–992.

Henderson, R., and P. N. T. Unwin. 1975. Three-dimensional model of purple membrane obtained by electron microscopy. *Nature (Lond.).* 257:28–32.

Herrmann, T. R., and G. W. Rayfield. 1978. The electrical response to light of bacteriorhodopsin in planar membranes. *Biophys. J.* 21:111–125.

Holz, M., M. Lindau, and M. P. Heyn. 1988. Distributed kinetics of the charge movements in bacteriorhodopsin: evidence for conformational substates. *Biophys. J.* 53:623–633.

Keszthelyi, L., and P. Ormos. 1980. Electric signals associated with the photocycle of bacteriorhodopsin. *FEBS (Fed. Eur. Biochem. Soc.) Lett.* 109:189–193.

Korenstein, R., B. Hess, and D. Kuschmitz. 1978. Branching reactions in the photocycle of bacteriorhodopsin. *FEBS (Fed. Eur. Biochem. Soc.) Lett.* 93:266–270.

Läuger, P. 1984. Thermodynamic and kinetic properties of electrogenic ion pumps. *Biochim. Biophys. Acta.* 779:307–341.

Liu, S. Y., and T. G. Ebrey. 1988. Photocurrent measurements of the purple membrane oriented in a polyacrylamide gel. *Biophys. J.* 54:321–329.

Oesterhelt, D., and W. Stoeckenius. 1974. Isolation of the cell membrane of Halobacterium halobium and its fractionation into red and purple membrane. *Methods Enzymol.* 31:667–678.

Quintanilha, A. T. 1980. Control of the photocycle in bacteriorhodopsin by electrochemical gradients. *FEBS (Fed. Eur. Biochem. Soc.) Lett.* 117:8–12.

Stoeckenius, W., R. H. Lozier, and R. A. Bogomolni. 1979. Bacteriorhodopsin and the purple membrane of halobacteria. *Biochim. Biophys. Acta.* 505:215–278.

Trissl, H.-W., and M. Montal. 1977. Electrical demonstration of rapid light-induced conformational changes in bacteriorhodopsin. *Nature (Lond.).* 266:655–657.

Váró, G., and L. Keszthelyi. 1983. Photoelectric signals from dried oriented purple membranes of *Halobacterium halobium. Biophys. J.* 43:47–51.

Watters, J., D. Kuschmitz, and B. Hess. 1982. Coupling of the photocycle and proton current in bacteriorhodopsin: a regulated phenomenon. *Hoppe-Seyler's Z. Physiol. Chem.* 363:549*a* (Abstr.)

Xie, A. H., J. F. Nagle, and R. H. Lozier. 1987. Flash spectroscopy of purple membrane. *Biophys. J.* 51:627–635.